Self-Propagating High-Temperature Synthesis
Самораспространяющийся высокотемпературный синтез

UDC 544.452 + 621.762.2 + 666.3
https://doi.org/10.17073/1997-308X-2025-5-36-50

Research article
Научная статья

Polytetrafluoroethylene-activated azide self-propagating high-temperature synthesis of a highly dispersed TiN–SiC powder composition

I. A. Uvarova[1], A. P. Amosov[1] ✉, Yu. V. Titova[1], A. A. Ermoshkin[2]

[1] Samara State Technical University
244 Molodogvardeiskaya Str., Samara 443100, Russia
[2] IT-Service LLC
52/55 Ulyanovskaya/Yarmarochnaya Str., Samara 443001, Russia

✉ egundor@yandex.ru

Abstract. Silicon carbide (SiC) and titanium nitride (TiN) are widely used non-oxide ceramics characterized by low density and high melting point, hardness, wear resistance, high-temperature strength, and corrosion resistance. However, single-phase silicon carbide ceramics have a number of drawbacks that limit their wider application. The main reason for developing TiN–SiC composite ceramics lies in the introduction of an electrically conductive TiN phase into the electrically non-conductive silicon carbide phase, which makes it possible to significantly reduce the high specific electrical resistivity of SiC while improving the sinterability, as well as the physical and mechanical properties of SiC-based composite ceramics. This study focuses on improving a simple and energy-efficient method of azide self-propagating high-temperature synthesis (SHS) for producing highly dispersed (<1 μm) TiN–SiC powder compositions from charge mixtures consisting of sodium azide (NaN_3), titanium, silicon, and carbon powders, through the use of powdered polytetrafluoroethylene (PTFE) as an activating and carbiding additive. The bulk and pressed charges were combusted in a reactor under a nitrogen pressure of 3 MPa. The maximum pressure and the yield of solid combustion products were measured. The morphology and phase composition of the combustion products were determined using scanning electron microscopy (SEM) and *X*-ray diffraction (XRD). The use of the PTFE additive eliminated the shortcomings of the traditional azide SHS of TiN–SiC compositions involving halide salts ($(NH_4)_2TiF_6$, Na_2SiF_6, and $(NH_4)_2SiF_6$). While maintaining the high dispersity of the synthesized TiN–SiC powder compositions, their phase composition became much closer to the theoretical one: the silicon carbide content in the synthesized TiN–SiC product increased substantially, while the amount of the secondary phase of silicon nitride (Si_3N_4) decreased or was completely eliminated.

Keywords: titanium nitride, silicon carbide, powder compositions, self-propagating high-temperature synthesis (SHS), sodium azide, polytetrafluoroethylene (PTFE), combustion products, composition, structure

Acknowledgements: The work was supported by the Russian Science Foundation under grant No. 23-29-00680.

For citation: Uvarova I.A., Amosov A.P., Titova Yu.V., Ermoshkin A.A. Polytetrafluoroethylene-activated azide self-propagating high-temperature synthesis of a highly dispersed TiN–SiC powder composition. *Powder Metallurgy and Functional Coatings*. 2025;19(5):36–50. https://doi.org/10.17073/1997-308X-2025-5-36-50

Применение политетрафторэтилена в азидном самораспространяющемся высокотемпературном синтезе высокодисперсной смеси керамических порошков TiN–SiC

И. А. Уварова[1], А. П. Амосов[1] ✉, Ю. В. Титова[1], А. А. Ермошкин[2]

[1] Самарский государственный технический университет
Россия, 443100, г. Самара, ул. Молодогвардейская, 244
[2] ООО «ИТ-Сервис»
Россия, 443001, г. Самара, ул. Ульяновская/Ярмарочная, 52/55

✉ egundor@yandex.ru

Аннотация. Карбид кремния (SiC) и нитрид титана (TiN) относятся к широко используемым неоксидным керамическим материалам с малой плотностью и высокими значениями температуры плавления, твердости, износостойкости, жаропрочности, коррозионной стойкости. Однако керамика из однофазного карбида кремния имеет ряд недостатков, препятствующих ее более широкому применению. Наиболее важная причина создания композиционной керамики TiN–SiC заключается в добавлении электропроводной фазы TiN в неэлектропроводную фазу карбида кремния для существенного снижения его высокого удельного электрического сопротивления с улучшением при этом спекаемости, физических и механических свойств композиционной керамики на основе SiC. Работа посвящена усовершенствованию простого энергосберегающего метода азидного самораспространяющегося высокотемпературного синтеза (СВС) композиций высокодисперсных (<1 мкм) порошков TiN–SiC из смесей исходных порошковых реагентов (шихт) азида натрия (NaN_3), титана, кремния и углерода за счет использования активирующей и карбидизирующей добавки порошкового политетрафторэтилена (ПТФЭ). Эти шихты в насыпном и прессованном виде сжигались в реакторе с давлением газообразного азота 3 МПа. Измерялись максимальное давление и выход твердых продуктов горения. С применением сканирующей электронной микроскопии и рентгенофазового анализа определялись морфология и фазовый состав продуктов горения. Использование добавки ПТФЭ позволило устранить недостатки традиционного азидного СВС композиций TiN–SiC с применением галоидных солей $(NH_4)_2TiF_6$, Na_2SiF_6 и $(NH_4)_2SiF_6$. При сохранении высокой дисперсности синтезированных композиций порошков TiN–SiC их фазовый состав стал значительно ближе к теоретическому составу, существенно увеличилось содержание карбида кремния в синтезированном продукте TiN–SiC при уменьшении содержания или полном устранении примеси побочной фазы нитрида кремния Si_3N_4.

Ключевые слова: нитрид титана, карбид кремния, композиции порошков, самораспространяющийся высокотемпературный синтез, азид натрия, политетрафторэтилен, продукты горения, состав, структура

Благодарности: Работа выполнена при поддержке Российского научного фонда в рамках гранта № 23-29-00680.

Для цитирования: Уварова И.А., Амосов А.П., Титова Ю.В., Ермошкин А.А. Применение политетрафторэтилена в азидном самораспространяющемся высокотемпературном синтезе высокодисперсной смеси керамических порошков TiN–SiC. *Известия вузов. Порошковая металлургия и функциональные покрытия*. 2025;19(5):36–50.
https://doi.org/10.17073/1997-308X-2025-5-36-50

Introduction

Silicon carbide (SiC) is one of the most widely used non-oxide ceramic materials due to its low density (3100 kg/m^3) and high values of such properties as melting point (refractoriness), hardness, wear resistance, thermal conductivity, dimensional thermal stability, high-temperature strength, heat resistance, and corrosion resistance. As a result, its application range extends from traditional uses – abrasive and cutting tool materials, mechanical seals, brake discs, turbine components, catalyst supports, heating elements, carbon and silicon sources for steelmaking, filters for molten metals and gases, and foundry crucibles – to modern applications such as composite armor for military vehicles and bulletproof vests, semiconductor processing components, mirror substrates for astronomical telescopes and other optical systems, matrices and claddings for nuclear fuel particles, and power electronic devices [1; 2].

However, single-phase silicon carbide ceramics have several drawbacks that limit their practical use [3]. First, SiC exhibits relatively low flexural strength (on average 450 MPa) and fracture toughness (2.8 MPa·m$^{1/2}$), which makes it brittle under impact loading. It is generally believed that increasing impact strength would enable silicon carbide to compete with structural materials based on silicon nitride, which exhibit higher flexural strength (around 750 MPa) and fracture toughness (approximately 5.3 MPa·m$^{1/2}$) [4; 5]. Second,

the extremely high melting point of silicon carbide (2730–2830 °C, with decomposition) caused by strong covalent bonding and low atomic self-diffusion results in poor sinterability of SiC powders. Therefore, very high temperatures of 2100–2200 °C are required during pressureless solid-state sintering, which leads to a coarser microstructure and deterioration of mechanical properties [4; 6]. Third, the high specific electrical resistivity of silicon carbide (10^6–10^{11} Ω·cm), typical of a semiconductor, prevents the fabrication of complex-shaped components by the cost-effective method of electrical discharge machining (EDM). Instead, mechanical machining of high-hardness SiC (20–30 GPa) requires expensive diamond tools, which also restricts its broader application [4; 7]. Moreover, when SiC ceramics are used as the friction pair in mechanical face seals, the specific (volume) electrical resistivity must be below ~10^3 Ω·cm to prevent triboelectric charge accumulation generated by rubbing of the mating end-faces during operation, which can trigger electrochemical corrosion and accelerate wear [8].

To date, extensive efforts have been made to overcome the aforementioned drawbacks of single-phase SiC ceramics by introducing secondary-phase additives, applying various processing and sintering technologies, using silicon carbide powders of different polytypes (α-SiC and β-SiC modifications) and dispersities, as well as adopting other approaches [1–9]. As a result, the most effective solution has been found to be the incorporation of secondary phases, i.e., the transition from single-phase SiC ceramics to SiC-based composite ceramics. Numerous studies have demonstrated that the addition of oxide, carbide, boride, and nitride phases enhances the sinterability and improves the physical and mechanical properties of SiC-based ceramics [6; 9].

Two main sintering methods for SiC ceramics involving additives are solid-state sintering and liquid-phase sintering. Solid-state sintering requires additives that reduce the energy barrier for SiC densification [6]. Carbon, boron, aluminum, titanium carbide (TiC), boron carbide (B_4C), and titanium diboride (TiB_2) are among the most widely used additives in this system [8–13]. However, even with these additives, the sintering temperature remains high, and achieving full densification of SiC continues to be a challenging task [6; 9]. Moreover, SiC ceramics containing carbon or graphene are unsuitable for semiconductor-processing components because carbon contamination adversely affects subsequent chemical vapor deposition (CVD) procedures. Similarly, aluminum-containing additives may be get into finished semiconductor products and worsen their performance characteristics [7].

Liquid-phase sintering is the most common method for producing SiC components. A liquid phase promotes faster mass transport, shortens sintering time, and lowers the sintering temperature to 1800–1900 °C [4; 6]. The final product generally exhibits a homogeneous, fine-grained microstructure and acceptable physical and mechanical properties. A widely used additive is an alumina–yttria mixture with the $5Al_2O_3{:}3Y_2O_3$ stoichiometry; under sintering conditions it forms a transient liquid that crystallizes to yttrium aluminum garnet (YAG, $Al_5Y_3O_{12}$), promoting densification and lowering the sintering temperature. Consequently, YAG formation increases density and enhances the mechanical properties of SiC ceramics through several toughening mechanisms, including crack deflection, crack bridging, phase transformation, grain-boundary strengthening, and a shift of the fracture mode from intergranular to transgranular [6]. In recent years, in addition to the Al_2O_3–Y_2O_3 system, other additives have been used to further improve the mechanical and physical properties and refine the microstructure of SiC-based ceramics. These include MgO, CaO, TiO_2, La_2O_3, and SiO_2 from the oxide group; TiC from the carbide group; TiB_2 and ZrB_2 from the boride group; and AlN and TiN from the nitride group [4; 6; 9]. Each of these additives imparts specific characteristics to SiC ceramics, generally inhibiting matrix grain growth, enhancing mechanical performance, and activating toughening mechanisms.

One of the most promising approaches for producing SiC ceramics suitable for electrical discharge machining is nitrogen doping (N-doping) of the SiC crystal lattice [7]. Nitrogen doping through the liquid phase can reduce the specific (volume) electrical resistivity of sintered SiC ceramics by up to ten orders of magnitude (from 10^8 to 10^{-2} Ω·cm) [14]. N-doping can be achieved either by sintering in a nitrogen atmosphere or by introducing nitride additives as a nitrogen source. However, gaseous N_2 inhibits mass transport and results in low density of sintered SiC ceramics [15], making the use of nitride-phase additives more promising. Importantly, adding 1 wt. % AlN lowers the specific (volume) electrical resistivity of SiC ceramics by four orders of magnitude – from $1.7\cdot10^5$ to $8.3\cdot10^1$ Ω·cm – but introduces undesirable aluminum impurities into the SiC matrix [16]. In contrast, the addition of 50 vol. % TiN decreases the specific electrical resistivity by nine orders of magnitude – from $2.0\cdot10^5$ Ω·cm (0 % TiN) to $2.0\cdot10^{-4}$ Ω·cm in the SiC–50 vol. % TiN composite – due to the combined beneficial effects of N-doping and the electrically conductive TiN grain boundaries [4; 17].

Given these considerations, let us focus more closely on the use of titanium nitride (TiN) powder as an additive – that is, on TiN–SiC ceramic composites. Like silicon carbide, titanium nitride has a high melting point (2950 °C), good corrosion resistance, and rela-

tively high hardness (20 GPa). However, TiN differs fundamentally from SiC in its very low specific electrical resistivity ($2.2 \cdot 10^{-5}$ Ω·cm) [18]. This key distinction determines the main interest in using an electrically conductive TiN ceramic phase as an additive to the non-conductive SiC ceramic matrix – to significantly reduce its high specific electrical resistivity (10^6–10^{11} Ω·cm) to below 10^3 Ω·cm, while simultaneously improving the sinterability and the physical and mechanical properties of SiC-based ceramics [6; 7; 9].

The first studies in this area investigated the effect of nano-TiN additions on sintering behavior, microstructure, and mechanical properties of SiC ceramics [19; 20]. A powder mixture consisting of α-SiC (particle size 0.5–1.0 μm) as the matrix, 0–15 wt. % TiN nanoparticles (average particle size 20 nm) as the reinforcing phase, and 10 wt. % of sintering additives ($5Al_2O_3 + 3Y_2O_3$) was cold-isostatically pressed at 250 MPa into rectangular bars and subsequently liquid-phase-sintered at 1950 °C for 15 min and then at 1850 °C for 1 h [19]. It was shown that the addition of TiN nanoparticles suppressed grain growth in the ceramics, and that reactions of TiN with SiC and of Al_2O_3 with the formation of new TiC and AlN phases, within a certain range of TiN content, improved the properties of SiC ceramics. The composition containing 5 wt. % nano-TiN exhibited the most homogeneous microstructure, the highest density, and a flexural strength of 686 MPa. The beneficial effect of nano-TiN addition was also demonstrated in another study [20] for pressureless-sintered SiC ceramics: the Vickers hardness increased from 18.19 to 26.65 GPa, flexural strength varied from 416 to 1122.81 MPa, and the maximum fracture toughness reached 8.69 MPa·$m^{1/2}$.

However, later research indicated that the use of nanopowders in fabricating SiC-based ceramics complicates processing and increases production costs due to the high price of the initial nanopowders [4; 13; 21]. Therefore, studies began to employ coarser and more affordable highly dispersed TiN powders with particle sizes up to 1 μm. SiC-based ceramic samples were produced by hot pressing at 2000 °C for 3 h under a nitrogen gas pressure of 40 MPa from a powder mixture of β-SiC (~0.5 μm), 2 or 4 vol. % TiN (~1 μm), and 2 vol. % Y_2O_3 as a sintering aid [21]. Phase-composition and microstructural analyses of the sintered samples revealed predominantly β-SiC grains with traces of α-SiC and Ti_2CN clusters located between β-SiC grains. The highly conductive *in-situ*-formed Ti_2CN clusters significantly reduced the specific electrical resistivity of the SiC ceramics to $2.4 \cdot 10^{-3}$ and $1.8 \cdot 10^{-4}$ Ω·cm for 2 and 4 vol. % TiN, respectively. In a subsequent study by the same group [17], SiC–Ti_2CN composites were fabricated by pressureless sintering at 1950 °C in a nitrogen atmosphere from powder mixtures containing 0, 3, 12, 20, and 25 vol. % TiN. All ceramic composite samples were sintered to a density of at least 98 % of the theoretical value, and their specific electrical resistivity decreased with increasing TiN content, reaching a minimum of $8.6 \cdot 10^{-4}$ Ω·cm at 25 vol. % TiN. The high electrical conductivity of the composites was attributed to *in-situ* synthesis of the conductive Ti_2CN phase and to grain growth of nitrogen-doped SiC during pressureless sintering. The sample containing 25 vol. % TiN exhibited a flexural strength of 430 MPa, fracture toughness of 4.9 MPa·$m^{1/2}$, and Vickers hardness of 23.1 GPa at room temperature.

In [4], SiC-based ceramic composites were fabricated by hot pressing at 1900 °C from SiC powder (~0.7 μm) with various TiN contents (0–50 wt. %, 0.8–1.2 μm), using Al_2O_3 and Y_2O_3 as sintering additives. The resulting composites reached densities above 98 % of the theoretical value. The specific electrical resistivity decreased from $2.0 \cdot 10^5$ Ω·cm (0 % TiN) with increasing TiN content and reached a plateau at $2.0 \cdot 10^{-4}$ Ω·cm for 40–50 wt. % TiN. At the same time, flexural strength gradually increased with the TiN content, attaining a maximum of 921 MPa at 40 wt. % TiN compared with 616 MPa for the original SiC (0 % TiN).

Additional results on the use of TiN additives were obtained for SiC ceramics produced by solid-state pressureless sintering in a graphite resistance furnace at a significantly higher temperature of 2100 °C for 2 h in a flowing argon atmosphere. The samples were prepared from pre-pressed powder mixtures of α-SiC (~0.5 μm) + 1–10 wt. % TiN (~1 μm) + 2.5 % C + 0.7 % B_4C (~0.5 μm) [7]. A TiN content up to 1 wt. % resulted in relative densities above 97 %, whereas further increase in TiN concentration led to the formation of large residual pores and a sharp decrease in relative density. For example, at ≥5 wt. % TiN, the density dropped to about 60 %, presumably due to the detrimental effect of excessive N_2 evolution during TiN decomposition. Nitrogen doping derived from TiN reduced the specific electrical resistivity by only one order of magnitude – to $9.0 \cdot 10^6$ Ω·cm at 1 wt. % TiN.

Thus, the effect of TiN addition on the properties of SiC-based ceramics strongly depends on the fabrication method, the composition of the initial powder mixtures, and the amount of TiN added. The most positive results – namely, a substantial decrease in specific electrical resistivity and improvement of mechanical properties – were achieved by hot pressing and pressureless sintering in a nitrogen atmosphere at temperatures not exceeding 2000 °C, using mixtures of highly

dispersed SiC and TiN powders (≤1–2 μm) with Al_2O_3 and Y_2O_3 as sintering additives and TiN contents from 1 to 50 wt. %.

In all the above studies, SiC–TiN ceramic composites were produced using the simplest and most common *ex situ* approach, which involves mechanical mixing of pre-synthesized SiC and TiN powders, followed by compaction and sintering. However, fine ceramic powders are costly; for instance, industrial-scale production of highly dispersed TiN powders requires complex equipment and energy-intensive plasma-chemical or vapor-phase reduction processes, in which titanium tetrachloride vapors are reduced by ammonia at 900–1000 °C [22; 23]. Furthermore, pre-synthesized fine powders are difficult to mix mechanically into a homogeneous composition because their particles tend to form strong agglomerates that are hard to break apart. For these reasons, an *in-situ* approach – based on the chemical synthesis of SiC and TiN powder particles directly within the composite from inexpensive starting reagents with uniform mixing – is considered more promising for the production of highly dispersed SiC–TiN composite powders [24–26]. To be fair, *in-situ* methods are currently used only under laboratory conditions and have not yet been adopted in industrial practice, where single-phase ceramic powders are still manufactured and composite powders are obtained by the traditional *ex-situ* route of mechanical mixing and milling of their single-phase components [25; 26]. Nevertheless, *in-situ* chemical synthesis methods for composite highly dispersed powders are considered advanced and strategically important, warranting further development and industrial implementation. Once this goal is achieved, high-quality composite highly dispersed powders will become commercially available, leading to significant improvements in the performance characteristics of the resulting composite ceramics [25; 26].

Among *in-situ* chemical synthesis methods for producing highly dispersed ceramic powders and their composites, the self-propagating high-temperature synthesis (SHS) method stands out for its simplicity and energy efficiency. It is based on the combustion of mixtures of inexpensive starting reagents [27–29]. Reference [29] presents earlier results, obtained with the participation of the present authors, on the application of the azide variant of SHS to Si–Ti–C–NaN_3–halide-salt systems. The charge mixtures consisted of silicon (Si), titanium (Ti), technical carbon (C), and sodium azide (NaN_3) as the nitriding reagent, with halide salts – $(NH_4)_2TiF_6$, Na_2SiF_6, and $(NH_4)_2SiF_6$ – serving as activating and gasifying additives. To synthesize highly dispersed TiN–SiC powder compositions at five molar ratios of the target phases – TiN:SiC = 4:1, 2:1, 1:1, 1:2, and 1:4 – the corresponding stoichiometric equations were formulated, for example

$$2Si + Ti + 6NaN_3 + (NH_4)_2TiF_6 + 2C =$$
$$= 2TiN + 2SiC + 6NaF + 4H_2 + 9N_2.$$

Of the 15 stoichiometric equations derived, only one is shown here for brevity – the equation using the halide salt $(NH_4)_2TiF_6$ corresponding to the TiN:SiC = 1:1 molar ratio of the target phases. The charge mixtures of the starting reagents corresponding to these 15 stoichiometries were combusted in bulk in an azide SHS reactor under a nitrogen pressure of 4 MPa. After cooling, the combustion products were removed from the reactor, disintegrated to a bulk powder form in a porcelain mortar, and washed with water to remove the by-product sodium fluoride (NaF). In most cases, the combustion product was a highly dispersed powder of complex composition, consisting of a mixture of submicron (0.1–1.0 μm) equiaxed particles and fibers. The phase composition of the washed combustion products is summarized in Table 1, in comparison with the theoretical composition of the TiN–SiC target phases at various molar ratios according to the 15 stoichiometric equations.

According to Table 1, the phase compositions of the synthesized TiN–SiC powders differed markedly from the theoretical predictions. The content of silicon carbide was much lower – or even absent – ranging from 0 to 49.4 wt. % instead of the theoretical 13.9–72.1 wt. %. In addition, a considerable amount of the secondary silicon nitride phase (12.3–54.2 wt. %) in α- and β-modifications was observed, despite its absence in the theoretical composition. The formation of SiC was especially limited, or completely suppressed, when the halide salt $(NH_4)_2TiF_6$ was used. It is also noteworthy that the azide SHS products contained only minor amounts of free silicon and carbon (≤1.4 wt. %) or none at all.

Reference [29] also reports that using the traditional azide SHS route with gasifying halide activators – $(NH_4)_2SiF_6$, AlF_3, and NH_4F – to synthesize AlN–SiC powders led to systematic deviations between the experimental and theoretical phase compositions across AlN:SiC molar ratios of 4:1, 2:1, 1:1, 1:2, and 1:4. On average, the SiC content was approximately half of the theoretical value, and substantial amounts of the undesired secondary phase Si_3N_4 were detected. These issues were recently addressed in our study [30] by replacing the halide activators with powdered polytetrafluoroethylene (PTFE, $(C_2F_4)_n$) used as an activating carbiding additive in the azide SHS synthesis of AlN–SiC powders. Partially substituting 0.1 mol of carbon with 0.05 mol of PTFE in the carbiding mixture ($0.9C + 0.05C_2F_4$), together with sodium azide as

the activating nitriding agent in an amount sufficient to neutralize the fluorine released upon complete PTFE decomposition, preserved the high dispersity of the synthesized AlN–SiC powders and brought their phase composition – particularly for pressed charges – much closer to the theoretical one. The SiC phase fraction increased substantially, and the undesired silicon nitride phases were eliminated.

A similar approach – partial substitution of 0.3 mol of carbon with 0.15 mol of PTFE in the carbiding mixture ($0.7C + 0.15C_2F_4$) – was used in our recently published work [31] to synthesize highly dispersed Si_3N_4–SiC powder compositions by azide SHS, yielding a phase composition close to the theoretical stoichiometry.

Considering these results, in the present study – aiming to bring the composition of the synthesized highly dispersed TiN–SiC powder mixture closer to the theoretical one by increasing the SiC phase content and removing the undesired secondary Si_3N_4 phase – we analogously used partial substitution of carbon with PTFE, instead of halide salt additives, in the initial Azide SHS reagent mixture, and investigated the combustion products of the Si–Ti–NaN_3–C–C_2F_4 system.

Research methodology

The following starting reagents were used in the study (hereafter in wt. %): silicon powder, grade Kr00 (main component ≥99.9 %, mean particle size d = 40 μm); titanium powder, grade PTOM-1 (98.0 %, d = 30 μm); sodium azide powder, analytical grade (≥98.71 %, d = 100 μm); polytetrafluoroethylene (PTFE) powder, grade PN-40 (≥99.0 %, d = 40 μm); and technical carbon black, grade P701 (≥88.0 %, d = 70 nm, agglomerates up to 1 μm).

As in [30; 31] and following [32; 33], to increase the silicon carbide content in the synthesized TiN–SiC composites, technical carbon was partially replaced by PTFE in amounts of 5, 10, and 15 %. This corresponded to the following carbiding mixtures of carbon and PTFE, each equivalent to one mole of carbiding carbon:

$$0.9C + 0.05C_2F_4, \quad (A)$$

$$0.8C + 0.1C_2F_4, \quad (B)$$

$$0.7C + 0.15C_2F_4. \quad (C)$$

Table 1. **Theoretical and experimental phase composition of washed solid products of azide SHS of the TiN–SiC composition [29]**

Таблица 1. **Теоретический и экспериментальный фазовые составы промытых твердых продуктов азидного СВС композиции TiN–SiC [29]**

TiN:SiC (mol)	Content, wt. %							
	Theoretical		Experimental					
	TiN	SiC	TiN	SiC	α-Si_3N_4	β-Si_3N_4	Si	C
Halide salt $(NH_4)_2TiF_6$								
4:1	86.1	13.9	87.7	–	5.6	6.7	–	–
2:1	75.6	24.4	80.0	–	14.0	6.0	–	–
1:1	60.7	39.3	45.8	–	49.8	4.4	–	–
1:2	43.6	56.4	41.2	6.4	43.9	7.6	0.9	–
1:4	27.9	72.1	28.8	19.9	42.5	7.4	1.4	–
Halide salt $(NH_4)_2SiF_6$								
4:1	86.1	13.9	61.0	4.0	27.0	7.0	1.0	–
2:1	75.6	24.4	71.0	–	18.0	9.0	1.2	0.8
1:1	60.7	39.3	54.7	16.0	17.4	11.9	–	–
1:2	43.6	56.4	40.0	31.0	19.0	9.0	1.0	–
1:4	27.9	72.1	24.2	49.4	21.1	5.0	0.3	–
Halide salt Na_2SiF_6								
4:1	86.1	13.9	76.0	–	19.0	5.0	–	–
2:1	75.6	24.4	64.0	10.0	17.0	9.0	–	–
1:1	60.7	39.3	54.0	20.0	15.0	11.0	–	–
1:2	43.6	56.4	42.0	34.0	16.0	8.0	–	–
1:4	27.9	72.1	23.0	49.0	21.0	6.0	1.0	–

Sodium azide (NaN_3) was added to the charge in an amount sufficient to neutralize the fluorine released during complete PTFE decomposition and to bind it into water-soluble sodium fluoride (NaF), which can be readily removed from the azide SHS product by washing with water. Consequently, the stoichiometric equations of azide SHS for the TiN–SiC target phases at five molar ratios (TiN:SiC = 4:1, 2:1, 1:1, 1:2, and 1:4) were derived for carbiding mixtures (*A*)–(*C*) containing PTFE, assuming combustion in gaseous nitrogen, as follows:

for carbiding mixture (*A*):

$$4Ti + Si + 0.9C + 0.05C_2F_4 + 0.2NaN_3 + 1.7N_2 = 4TiN + SiC + 0.2NaF, \quad (1)$$

$$2Ti + Si + 0.9C + 0.05C_2F_4 + 0.2NaN_3 + 0.7N_2 = 2TiN + SiC + 0.2NaF, \quad (2)$$

$$Ti + Si + 0.9C + 0.05C_2F_4 + 0.2NaN_3 + 0.2N_2 = TiN + SiC + 0.2NaF, \quad (3)$$

$$Ti + 2Si + 1.8C + 0.1C_2F_4 + 0.4NaN_3 = TiN + 2SiC + 0.4NaF + 0.1N_2, \quad (4)$$

$$Ti + 4Si + 3.6C + 0.2C_2F_4 + 0.8NaN_3 = TiN + 4SiC + 0.8NaF + 0.7N_2; \quad (5)$$

for carbiding mixture (*B*):

$$4Ti + Si + 0.8C + 0.1C_2F_4 + 0.4NaN_3 + 1.4N_2 = 4TiN + SiC + 0.4NaF, \quad (6)$$

$$2Ti + Si + 0.8C + 0.1C_2F_4 + 0.4NaN_3 + 0.4N_2 = 2TiN + SiC + 0.4NaF, \quad (7)$$

$$Ti + Si + 0.8C + 0.1C_2F_4 + 0.4NaN_3 = TiN + SiC + 0.4NaF + 0.1N_2, \quad (8)$$

$$Ti + 2Si + 1.6C + 0.2C_2F_4 + 0.8NaN_3 = TiN + 2SiC + 0.8NaF + 0.7N_2, \quad (9)$$

$$Ti + 4Si + 3.2C + 0.4C_2F_4 + 1.6NaN_3 = TiN + 4SiC + 1.6NaF + 1.9N_2; \quad (10)$$

for carbiding mixture (*C*):

$$4Ti + Si + 0.7C + 0.15C_2F_4 + 0.6NaN_3 + 1.1N_2 = 4TiN + SiC + 0.6NaF, \quad (11)$$

$$2Ti + Si + 0.7C + 0.15C_2F_4 + 0.6NaN_3 + 0.1N_2 = 2TiN + SiC + 0.6NaF, \quad (12)$$

$$Ti + Si + 0.7C + 0.15C_2F_4 + 0.6NaN_3 = TiN + SiC + 0.6NaF + 0.4N_2, \quad (13)$$

$$Ti + 2Si + 1.4C + 0.3C_2F_4 + 1.2NaN_3 = TiN + 2SiC + 1.2NaF + 1.3N_2, \quad (14)$$

$$Ti + 4Si + 2.8C + 0.6C_2F_4 + 2.4NaN_3 = TiN + 4SiC + 2.4NaF + 3.1N_2. \quad (15)$$

The reagent mixtures corresponding to equations (1)–(15), with masses ranging from 23 to 37 g (average 30 g), were combusted in a 4.5 L azide SHS reactor under an initial nitrogen pressure of P_0 = 3 MPa. Combustion was performed in two forms: as a bulk charge, placed in a tracing-paper crucible (30 mm in diameter and 45 mm in height), and as briquetted charges, compacted under 7 MPa into cylindrical pellets measuring 30 mm in diameter and approximately 22 mm in height. (The nitrogen pressure of 3 MPa and the briquette compaction pressure of 7 MPa for a 30 mm charge diameter were selected according to [33], which demonstrated that under these conditions partial replacement of carbon with PTFE ensures the complete course of the silicon carburization reaction and the formation of SiC particles with an average size of about 200 nm). Combustion was initiated using a tungsten spiral heater. The maximum gas pressure (P_{max}) in the reactor during combustion was recorded using a manometer. After cooling, the combustion products were removed from the reactor, disintegrated to a bulk powder form in a porcelain mortar, and washed with water to remove the byproduct sodium fluoride (NaF). The dried and washed combustion product was weighed, and the mass loss (Δm, %) was determined as the difference between the initial charge mass (m_0) and the mass of the washed product (m_k). This mass loss was interpreted as the scattering of part of the solid synthesis products beyond the charge volume due to gases intensively released during combustion. (This estimation of product scattering is approximate, since it does not account for the formation of NaF in the products or for the consumption or release of gaseous nitrogen in the reactor according to equations (1)–(15). However, because this approach was used in our previous studies [30; 31], it is retained here to ensure comparability of the product-scattering data. The validity of this estimation will be discussed later in the following sections of the paper).

The phase composition of the synthesized products was analyzed using an ARL X'TRA powder *X*-ray diffractometer (Thermo Fisher Scientific, Switzerland) equipped with a Cu anode *X*-ray tube. The diffraction patterns were processed, and the phase composition was determined by the Rietveld refinement method

using the HighScore Plus software package and the COD-2024 crystallographic database. The morphology and particle size of the synthesized powders were examined with a JSM-6390A scanning electron microscope (JEOL, Japan).

Results and discussion

The experimentally determined maximum reactor pressure (P_{max}), mass loss (Δm) for the bulk and pressed powder charges of reactions (1)–(15), and the phase compositions of the washed solid combustion products are summarized in Table 2 as average values from three repeated experiments for each charge.

A comparison between the experimental phase compositions of the washed solid products of the Azide SHS reactions for TiN–SiC compositions (Tables 1 and 2) reveals a marked difference between the two sets of results. Table 2 shows that partial substitution of technical carbon with PTFE led to the formation of a considerably higher fraction of silicon carbide (13–72 %), compared to the use of halide salts (0–49.4 % SiC, Table 1). Whereas some compositions in Table 1 show complete absence of SiC (0 %), all samples in Table 2 contained measurable SiC. Notably, the experimentally obtained SiC contents (13–72 %) in Table 2 are very close to their theoretical values (13.9–72.1 %) calculated from the stoichiometric equations. A similar trend is observed for the secondary silicon nitride (Si_3N_4) phase in α- and β-modifications. While the total Si_3N_4 content in Table 1 reached 12.3–54.2 %, its amount in Table 2 was much lower (0–18 %) and, in several cases, completely absent, in line with theoretical predictions. Table 2 also indicates that free carbon impurities were entirely absent, and free silicon was either undetected or present in trace amounts, not exceeding a few tenths of a percent. Only four of the thirty analyzed samples contained 1.0–3.3 % Si. Overall, the data in Table 2 show that the experimental phase compositions of the TiN and SiC target phases obtained via azide SHS using PTFE correspond much more closely to the theoretical stoichiometric predictions than those achieved by the traditional Azide SHS process with halide additives $(NH_4)_2TiF_6$, Na_2SiF_6, and $(NH_4)_2SiF_6$ [29].

However, Table 2 also shows very large mass losses (product scattering) during combustion, particularly for bulk charges (42.0–88.7 %), with noticeably lower values for pressed charges (17.7–77.5 %). In contrast, in traditional azide SHS processes, these values were much smaller – for example, 4.2–10.4 % for Si_3N_4–SiC synthesis from bulk charges using the halide salt NH_4F [34]. The mass losses observed here for TiN–SiC are also significantly higher than those reported for AlN–SiC compositions synthesized using carbiding mixture (*A*) with PTFE – 0.2–38.9 % for bulk charges and 0.1–26.3 % for pressed charges [30]. Meanwhile, the mass losses of the solid products obtained for mixture (*C*) are comparable to those reported for Si_3N_4–SiC synthesized with the same mixture – 57.0–81.4 % for bulk charges and 12.6–80.4 % for pressed charges [31].

We now consider how including NaF formation in the products and the consumption or release of gaseous nitrogen in the reactor affects the calculated mass loss of the combustion products. First, consider reaction (1), which consumes gaseous nitrogen, using a bulk charge that showed a large product-scattering loss of 73.5 % (Table 2). For this reaction, the charge mass was $m_0 = 37.23$ g, and the mass of the washed product was $m_k = 9.83$ g. On the right-hand side of equation (1), 0.2 NaF corresponds to 2.92 %, or 0.29 g, relative to the mass of 4TiN + SiC equal to 9.83 g. Thus, the unwashed product mass equals 10.12 g, and when the NaF mass is taken into account, the product mass loss decreases from 73.5 to 72.8 %. The correction for nitrogen consumption is made based on the left-hand side of equation (1), where 1.7 N_2 accounts for 19.13 %, or 7.12 g, of the total charge mass of 37.23 g. When the consumed nitrogen is taken into account, the total mass of the initial reactants on the left-hand side of equation (1) increases to 44.35 g. Consequently, the estimated mass loss of the unwashed product – including the NaF mass – rises from 72.8 to 77.2 %. Thus, accounting for the mass of NaF formed in the product and for the nitrogen consumed in the reactor changes the approximate product mass loss value of 73.5 % to more accurate estimates of 72.8 and 77.2 %, respectively. However, this difference is negligible at high product-loss levels.

For the average product loss value in Table 2 – an approximate estimate of 29.5 % for reaction (11) with a pressed charge – similar calculations show that accounting for NaF formation in the product and for the mass of nitrogen consumed yields more accurate product-loss estimates of 23.3 and 30.8 %, respectively. When only NaF formation is taken into account, the calculated value of 23.3 % is noticeably lower than the approximate estimate of 29.5 %; however, when both factors (NaF and N_2) are included, the resulting value of 30.8 % differs insignificantly from the approximate estimate of 29.5 %.

For the minimum scattering-related mass loss – an approximate estimate of 17.7 % for reaction (3) with a pressed charge – accounting only for NaF formation likewise gives a noticeably lower value of 10.9 %. However, when both NaF formation and nitrogen consumption are taken into account, the resulting value

Table 2. **Combustion parameters of charge mixtures for reactions (1)–(15) and theoretical and experimental phase compositions of washed solid products for bulk and pressed charges**

Таблица 2. **Параметры горения шихт реакций (1)–(15) и теоретический и экспериментальный фазовые составы промытых твердых продуктов реакций для насыпных и прессованных шихт**

Reaction equation	TiN:SiC (mol)	P_{max}, MPa	Δm, %	Phase composition of reaction products, wt. %							
				Theoretical		Experimental					
				TiN	SiC	TiN	SiC	α-Si_3N_4	β-Si_3N_4	Si	Other
Bulk charges											
Carbiding mixture (*A*)											
(1)	4:1	5.33	73.5	86.1	13.9	71.3	13.0	–	–	–	15.7 Ti_2N
(2)	2:1	5.49	77.1	75.6	24.4	74.1	23.3	–	–	0.4	2.2 Ti
(3)	1:1	5.18	63.5	60.7	39.3	59.4	37.3	–	–	3.3	–
(4)	1:2	4.60	83.5	43.6	56.4	28.0	55.0	10.0	6.0	1.0	–
(5)	1:4	4.44	78.1	27.9	72.1	29.0	51.0	13.0	5.0	2.0	–
Carbiding mixture (*B*)											
(6)	4:1	5.71	57.0	86.1	13.9	86.5	13.5	–	–	–	–
(7)	2:1	5.75	57.6	75.6	24.4	75.0	22.0	–	–	3.0	–
(8)	1:1	5.62	81.9	60.7	39.3	59.5	33.3	–	6.3	0.9	–
(9)	1:2	5.25	85.4	43.6	56.4	38.9	53.3	2.3	5.0	0.5	–
(10)	1:4	5.49	87.6	27.9	72.1	17.0	72.0	4.8	6.0	0.2	–
Carbiding mixture (*C*)											
(11)	4:1	5.04	42.0	86.1	13.9	81.7	15.2	3.1	–	–	–
(12)	2:1	5.87	69.5	75.6	24.4	75.8	22.1	2.1	–	–	–
(13)	1:1	5.87	88.7	60.7	39.3	57.3	34.0	5.0	3.3	0.4	–
(14)	1:2	5.98	69.5	43.6	56.4	37.2	55.7	4.0	3.1	–	–
(15)	1:4	4.91	78.2	27.9	72.1	25.0	69.0	4.0	2.0	–	–
Pressed charges											
Carbiding mixture (*A*)											
(1)	4:1	5.30	38.3	86.1	13.9	88.7	11.3	–	–	–	–
(2)	2:1	5.15	36.3	75.6	24.4	72.3	17.3	10.1	–	0.3	–
(3)	1:1	4.76	17.7	60.7	39.3	60.4	30.0	9.6	–	–	–
(4)	1:2	4.45	39.2	43.6	56.4	23.0	65.0	10.0	2.0	–	–
(5)	1:4	4.58	58.6	27.9	72.1	25.0	61.5	11.0	2.5	–	–
Carbiding mixture (*B*)											
(6)	4:1	4.58	49.7	86.1	13.9	84.5	15.5	–	–	–	–
(7)	2:1	5.67	48.1	75.6	24.4	72.7	27.0	–	–	0.3	–
(8)	1:1	5.45	32.9	60.7	39.3	60.4	33.1	6.0	–	0.5	–
(9)	1:2	5.23	49.3	43.6	56.4	40.0	53.0	4.0	3.0	–	–
(10)	1:4	5.47	74.2	27.9	72.1	21.9	67.6	6.5	4.0	–	–
Carbiding mixture (*C*)											
(11)	4:1	5.21	29.5	86.1	13.9	83.0	14.0	3.0	–	–	–
(12)	2:1	5.54	32.6	75.6	24.4	73.4	22.5	4.3	–	–	–
(13)	1:1	5.67	35.5	60.7	39.3	56.7	34.0	7.3	–	0.2	–
(14)	1:2	5.75	45.5	43.6	56.4	39.8	55.5	5.3	–	–	–
(15)	1:4	5.74	77.5	27.9	72.1	26.2	69.9	3.6	–	–	–

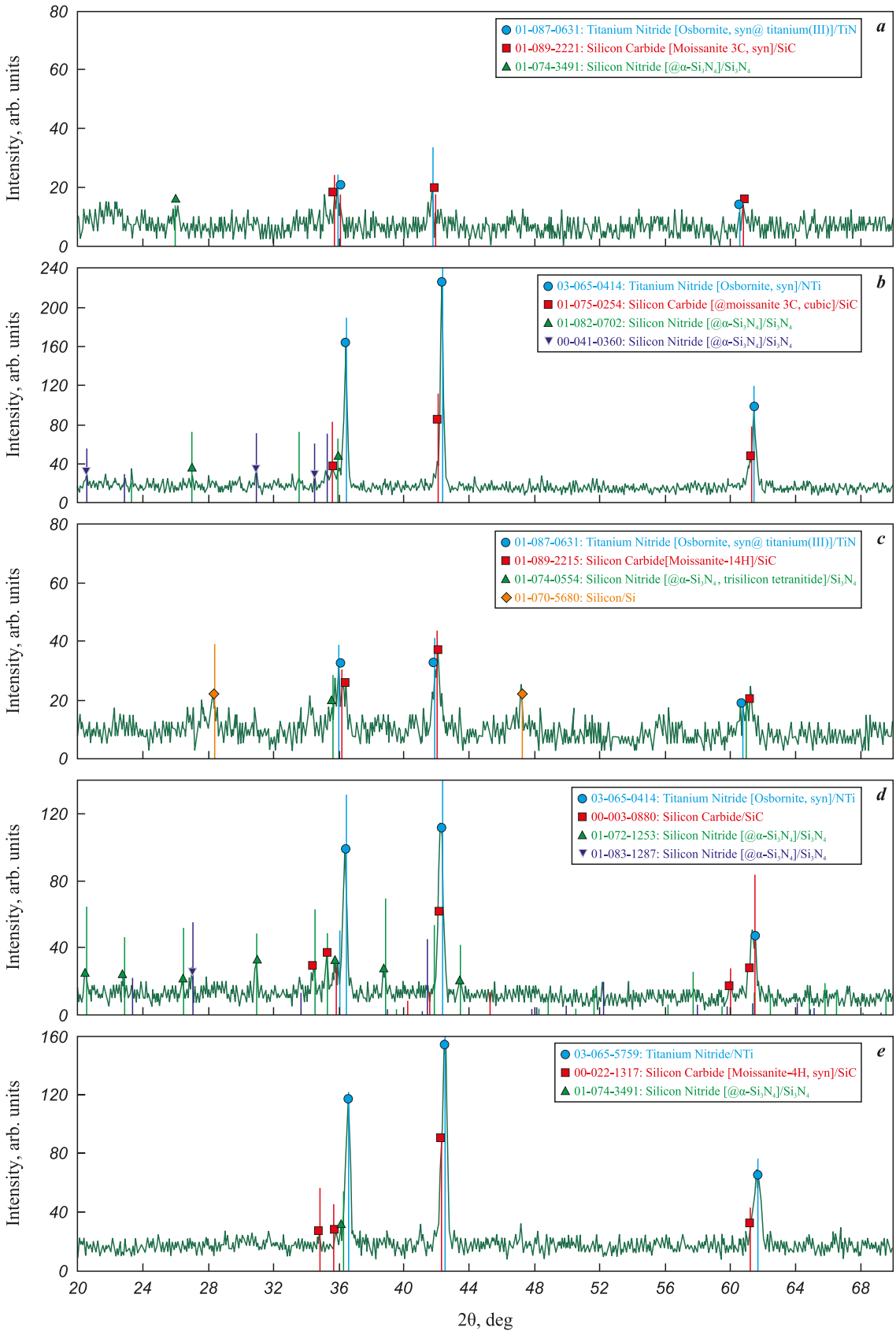

Fig. 1. XRD patterns of the washed combustion products of pressed charges from reaction equations (11)–(15)
a – (11), ***b*** – (12), ***c*** – (13), ***d*** – (14), ***e*** – (15)

Рис. 1. Рентгеновские дифрактограммы промытых продуктов горения прессованных шихт из уравнений реакций (11)–(15)
a – (11), ***b*** – (12), ***c*** – (13), ***d*** – (14), ***e*** – (15)

of 15.5 % differs only slightly from the approximate estimate of 17.7 %.

Thus, for reactions involving nitrogen consumption, the approximate estimates of solid product loss are close to the more accurate values obtained when both NaF formation and nitrogen consumption are fully taken into account, the latter increasing the total mass of the initial reactants. In contrast, for reactions accompanied by nitrogen release – where nitrogen appears on the right-hand side of the reaction equations – there is no need to consider it when evaluating the loss of solid products, since gaseous nitrogen is not part of the solid phase. In these cases, a more accurate loss estimate involves accounting only for NaF formation, whose mass is generally small compared with the other solid reaction products and can reduce the calculated loss value by approximately 10 %. For example, in reaction (8) from Table 2 (pressed charge), the approximate product loss is 32.9 %, while accounting for NaF formation gives 21.9 %. The relative difference between the two estimates is therefore significant (33.4 %), demonstrating how strongly NaF correction can reduce the calculated solid product loss in cases of small overall loss. Conversely, for reaction (15) with a very large product loss (approx. 77.5 %), accounting for NaF formation lowers the estimated loss to 67.3 %, where the relative difference is minor (13.2 %).

It was then necessary to select, from the 30 charge variants presented in Table 2, those corresponding to different TiN:SiC molar ratios that most closely matched the theoretical phase compositions calculated from the initial stoichiometric equations, while also exhibiting the lowest combustion-related losses. These optimal variants could then be recommended for further study and for assessing the feasibility of using the azide SHS process with PTFE to produce commercially viable highly dispersed TiN–SiC composite powders. The selection was based on a comparative assessment of the efficiency of bulk and pressed charges prepared with different carbiding mixtures (*A*, *B*, and *C*), using two parameters: the mass loss of the solid reaction products (Δm, %) and the total impurity content in these products (impurities, %). From the data in Table 2, the average values of these parameters for all variants were calculated as follows: for bulk charges, Δm = 72.9 % and impurities = 7.64 %; for pressed charges, Δm = 44.3 % and impurities = 6.22 %. Thus, in general, the use of bulk charges results in considerably higher product losses and greater contamination by impurities compared with pressed charges. Therefore, the search for the best synthesis conditions was continued among the pressed charges prepared with the three carbiding mixtures. Based on the results obtained with these mixtures (*A*, *B*, and *C*), the average

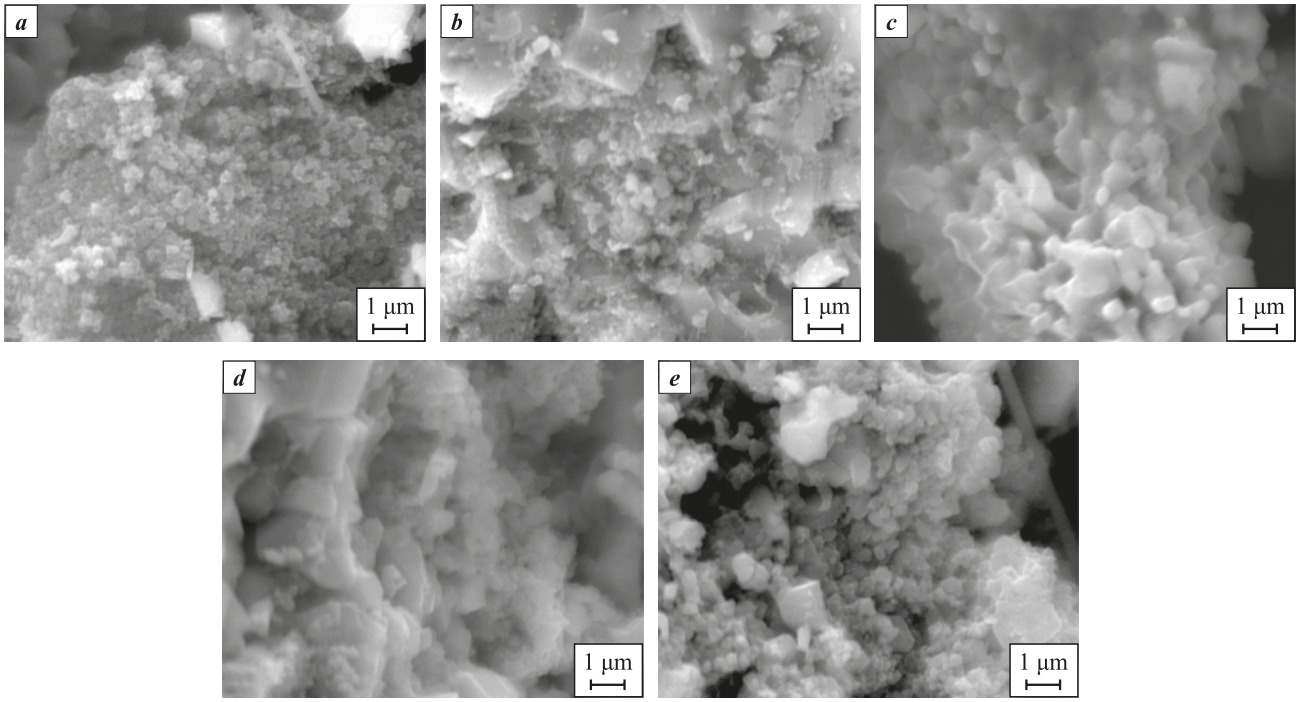

Fig. 2. SEM images of the washed combustion products of pressed charges from reaction equations (11)–(15)
a – (11), ***b*** – (12), ***c*** – (13), ***d*** – (14), ***e*** – (15)

Рис. 2. Морфология промытых продуктов горения прессованных шихт из уравнений реакций (11)–(15)
a – (11), ***b*** – (12), ***c*** – (13), ***d*** – (14), ***e*** – (15)

values of the parameters were as follows: Δm = 38.0 %, 50.8 %, and 44.1 %, and impurities = 9.1 %, 4.9 %, and 4.7 %, respectively. Mixture (*A*) provided the lowest mass loss (38.0 %) but also the highest impurity content (9.1 %). Mixture (*C*), in contrast, showed a slightly higher mass loss (44.1 %) yet a markedly lower impurity level (4.7 %), nearly twice as low as for mixture (*A*); therefore, mixture (*C*) was considered the most favorable option. Mixture (*B*) demonstrated a somewhat higher impurity level (4.9 %) and noticeably larger product losses (50.8 %) compared with mixture (*C*). Consequently, mixture (*C*) can be regarded as the most efficient carbiding composition for pressed charges. As a result of this systematic analysis, the best synthesis variants – those representing the optimal balance between product loss and impurity content – were identified for all five TiN:SiC molar ratios. These correspond to the pressed charges prepared with carbiding mixture (*C*) according to equations (11)–(15). Indeed, most of these variants exhibit some of the lowest product mass losses – 29.5, 32.6, 35.5, and 45.5 % for equations (11)–(14), respectively – and impurity levels of 3.0, 4.3, 5.3, and 3.6 % for equations (11), (12), (14), and (15), respectively. However, two issues remain: the relatively high impurity level (7.3 %) in the products of reaction (13) and the very large product loss (77.5 %) observed for reaction (15). These questions are discussed in the Conclusion section.

The *X*-ray diffraction patterns of the washed combustion products for the selected optimal synthesis variants of the TiN–SiC powder compositions are shown in Fig. 1.

The diffraction patterns in Fig. 1 exhibit strong reflections corresponding to the target phases TiN and SiC, along with weak reflections from minor impurities of free Si and secondary phases α-Si_3N_4 and β-Si_3N_4. In some cases, these impurity reflections are absent altogether. As seen from Fig. 1 and Table 2, silicon nitride forms predominantly in the α-Si_3N_4 modification.

The morphology of the TiN–SiC powder compositions for the selected best synthesis variants is presented in Fig. 2.

As shown in Fig. 2, all synthesized products are highly dispersed powders composed of equiaxed particles less than 1–2 μm in size, aggregated into agglomerates.

Conclusion

This study shows that replacing the halide activators $(NH_4)_2TiF_6$, Na_2SiF_6, $(NH_4)_2SiF_6$ with polytetrafluoroethylene (PTFE) as an activating, carbiding additive in azide SHS – together with partial substitution of technical carbon by 5–15 % – substantially increases the SiC phase fraction in the synthesized highly dispersed TiN–SiC powders, while reducing or completely eliminating the secondary Si_3N_4 phase. As a result, the experimental phase compositions obtained with PTFE agree much more closely with the theoretical stoichiometric predictions than those produced by the traditional azide SHS route using halide salts.

The drawback is that PTFE can lead to large mass losses of solid product (up to 88.7 %) due to scattering by vigorously evolving gases. Bulk charges showed higher losses on average (72.9 %) than pressed charges (44.3 %), and their products contained more impurities (average 7.64 % vs 6.22 %). The best balance of low loss and low impurity was achieved with 15 % PTFE replacing carbon in pressed charges across all five TiN:SiC ratios (4:1, 2:1, 1:1, 1:2, 1:4). The corresponding mass losses were 29.5, 32.6, 35.5, 45.5, 77.5 %, and the impurity contents were 3.0, 4.3, 5.3, 7.3, 3.6 %, respectively. These conditions are promising candidates for further study toward commercial production of composite, highly dispersed TiN–SiC powders by azide SHS with PTFE.

Further research should be conducted in pilot-scale SHS reactors (SHS-20 and SHS-30, with volumes of 20 and 30 L, respectively) capable of accommodating kilogram-scale charges, rather than in a small 4.5 L laboratory reactor limited to ≤50 g [27; 35]. Increasing the charge mass is expected to enhance self-heating during SHS, leading to a longer and higher thermal profile due to reduced specific heat losses from the surface compared with smaller charges (≤50 g). This effect should promote more complete formation of the TiN and SiC phases and reduce the total impurity content (Si + Si_3N_4) to well below 7.3 %. To reduce losses of the target powder products caused by scattering during vigorous gas evolution in combustion – reaching 77.5 % in one of the recommended variants – the charge should be placed in filtering assemblies when burned in pilot-scale reactors. These assemblies are hollow cylindrical frames made of metal mesh or thin steel sheet with numerous drilled perforations and gas-permeable inner liners of carbon fabric or fiberglass [35]. In addition, scattering-related mass loss can be further reduced by increasing the initial nitrogen pressure in the reactor. For example, in our previous study [31] on azide SHS of the Si_3N_4:SiC = 1:4 composition from a pressed PTFE-containing charge, raising the initial nitrogen pressure from 3 to 4 MPa led to a nearly twofold decrease in Δm – from 80.4 to 41.9 % – while maintaining a comparable phase composition of the washed combustion product. With these measures, scattering-related losses in the other recommended variants can be reduced to well below 30 %.

References / Список литературы

1. Kim Y.-W., Malik R. SiC ceramics, structure, processing and properties. In: *Encyclopedia of Materials: Technical Ceramics and Glasses*. Ed. M. Pomeroy. Oxford: Elsevier, 2021. Vol. 2. P. 150–164. https://doi.org/10.1016/B978-0-12-818542-1.00022-9
2. Ruys A.J. Silicon carbide ceramics. Structure, properties and manufacturing. 1st ed. Elsevier, 2023. 586 p.
3. Oguntuyi S.D., Nyembwe K., Shongwe M.B., Johnson O.T., Adewumi J.R., Malatji N., Olubambi P.A. Improvement on the fabrication of SiC materials: Processing, reinforcing phase, fabricating route – A review. *International Journal of Lightweight Materials and Manufacture*. 2023;6(2):225–237. https://doi.org/10.1016/j.ijlmm.2022.10.005
4. Wing Z.N. TiN modified SiC with enhanced strength and electrical properties. *Journal of the European Ceramic Society*. 2017;37(4):1373–1378. https://doi.org/10.1016/j.jeurceramsoc.2016.11.007
5. Bobovich B.B. Nonmetallic structural materials: Textbook. Moscow: MGIU, 2009. 384 p. (In Russ.).

   Бобович Б.Б. Неметаллические конструкционные материалы: Учеб. пос. М.: МГИУ, 2009. 384 с.
6. Khodaei M., Yaghobizadeh O., Alhosseini S.N., Esmaeeli S., Mousavi S.R. The effect of oxide, carbide, nitride and boride additives on properties of pressureless sintered SiC: A review. *Journal of the European Ceramic Society*. 2019;39(7):2215–2231. https://doi.org/10.1016/j.jeurceramsoc.2019.02.042
7. Malik R., Kim Y.W. Effect of nitride addition on the electrical and thermal properties of pressureless solid-state sintered SiC ceramics. *Journal of the Korean Ceramic Society*. 2022;59(5):589–594. https://doi.org/10.1007/s43207-022-00190-4
8. Cai N., Guo D., Wu G., Xie F., Tan S., Jiang N., Li H. Decreasing resistivity of silicon carbide ceramics by incorporation of graphene. *Materials*. 2020;13(16):3586. https://doi.org/10.3390/ma13163586
9. Faeghinia A. Comparing the effects of different sintering aids on spark plasma sintering of SiC ceramics. *Synthesis and Sintering*. 2024;4(2):79–86. https://doi.org/10.53063/synsint.2024.42187
10. Prochazka S., Scanlan R.M. Effect of boron and carbon on sintering of SiC. *Journal of the American Ceramic Society*. 1975;58(1-2):72. https://doi.org/10.1111/j.1151-2916.1975.tb18990.x
11. Sahani P., Karak S.K., Mishra B., Chakravarty D., Chaira D. Effect of Al addition on SiC–B_4C cermet prepared by pressureless sintering and spark plasma sintering methods. *International Journal of Refractory Metals and Hard Materials*. 2016;57:31–41. https://doi.org/10.1016/j.ijrmhm.2016.02.005
12. Zhang Z., Xu C., Du X., Li Z., Wang J., Xing W., Sheng Y., Wang W., Fu Z. Synthesis mechanism and mechanical properties of TiB_2–SiC composites fabricated with the B_4C–TiC–Si system by reactive hot pressing. *Journal of Alloys and Compounds*. 2015;619:26–30. https://doi.org/10.1016/j.jallcom.2014.09.030
13. Ahmoye D., Bucevac D., Krstic V.D. Mechanical properties of reaction sintered SiC–TiC composite. *Ceramics International*. 2018;44(12):14401–14407. https://doi.org/10.1016/j.ceramint.2018.05.050
14. Kim Y.W., Cho T.Y., Kim K.J. Efect of grain growth on electrical properties of silicon carbide ceramics sintered with gadolinia and yttria. *Journal of the European Ceramic Society*. 2015;35(15):4137–4142. https://doi.org/10.1016/j.jeurceramsoc.2015.08.006
15. Taki Y., Kitiwan M., Katsui H., Goto T. Effect of B doping on electrical and thermal properties of SiC bodies fabricated by spark plasma sintering. *Materials Today Proceedings*. 2019;16(1):211–215. https://doi.org/10.1016/j.matpr.2019.05.249
16. Malik R., Kim Y.W. Effect of AlN addition on the electrical resistivity of pressureless sintered SiC ceramics with B_4C and C. *Journal of the American Ceramic Society*. 2021; 104(12):6086–6091. https://doi.org/10.1111/jace.18003
17. Cho T.Y., Malik R., Kim Y.W., Kim K.J. Electrical and mechanical properties of pressureless sintered SiC–Ti_2CN composites. *Journal of the European Ceramic Society*. 2018;38(9):3064–3072. https://doi.org/10.1016/j.jeurceramsoc.2018.03.040
18. Samsonov G.V., Vinitskii I.M. Refractory compounds: Handbook. 2nd ed. Moscow: Metallurgiya, 1976. 558 p. (In Russ.).

   Самсонов Г.В., Виницкий И.М. Тугоплавкие соединения: Справочник. 2-е изд. М.: Металлургия, 1976. 558 с.
19. Guo X., Yang H., Zhang L., Zhu X. Sintering behavior, microstructure and mechanical properties of silicon carbide ceramics containing different nano-TiN additive. *Ceramics International*. 2010;36(1):161–165. https://doi.org/10.1016/j.ceramint.2009.07.013
20. Zhang L., Yang H., Guo X., Shen J., Zhu X. Preparation and properties of silicon carbide ceramics enhanced by TiN nanoparticles and SiC whiskers. *Scripta Materialia*. 2011;65(3):186–189. https://doi.org/10.1016/j.scriptamat.2011.03.034
21. Kim K.J., Lim K.-Y., Kim Y.-W. Electrically and thermally conductive SiC ceramics. *Journal of the Ceramic Society of Japan*. 2014;122(1431):963–966. https://doi.org/10.2109/jcersj2.122.963
22. Kiesler D., Bastuck T., Theissmann R., Kruis F.E. Plasma synthesis of titanium nitride, carbide and carbonitride nanoparticles by means of reactive anodic arc evaporation from solid titanium. *Journal of Nanoparticle Research*. 2015;17(3):152. https://doi.org/10.1007/s11051-015-2967-8
23. Dekker J.P., van der Put P.J., Veringa H.J., Schoonman J. Vapor-phase synthesis of titanium nitride powder. *Journal of Materials Chemistry*. 1994;4(5):689–694. https://doi.org/10.1039/JM9940400689
24. Basu B., Balani K. Advanced structural ceramics. Hoboken. New Jersey: John Wiley & Sons, Inc., 2011. 502 p.
25. Palmero P. Structural ceramic nanocomposites: A review of properties and powders' synthesis methods. *Nanomaterials*. 2015;5(2):656–696. https://doi.org/10.3390/nano5020656
26. Montanaro L., Palmero P. Advances in the field of nanostructured ceramic composites. *Ceramics*. 2019;2(2): 296–297. https://doi.org/10.3390/ceramics2020024

27. Rogachev A.S., Mukasyan A.S. Combustion for material synthesis. New York: CRC Press, 2014. 424 p. https://doi.org/10.1201/b17842

Рогачев А.С., Мукасьян А.С. Горение для синтеза материалов. М.: Физматлит, 2012. 400 с.

28. Levashov E.A., Mukasyan A.S., Rogachev A.S., Shtansky D.V. Self-propagating high-temperature synthesis of advanced materials and coatings. *International Materials Reviews*. 2016;62(4):1–37. https://doi.org/10.1080/09506608.2016.1243291

29. Amosov A.P., Titova Yu.V., Belova G.S., Maidan D.A., Minekhanova A.F. SHS of highly dispersed powder compositions of nitrides with silicon carbide. Review. *Powder Metallurgy and Functional Coatings*. 2022;16(4):34–57. https://doi.org/10.17073/1997-308X-2022-4-34-57

Амосов А.П., Титова Ю.В., Белова Г.С., Майдан Д.А., Минеханова А.Ф. СВС высокодисперсных порошковых композиций нитридов с карбидом кремния: Обзор. *Известия вузов. Порошковая металлургия и функциональные покрытия*. 2022;16(4):34–57. https://doi.org/10.17073/1997-308X-2022-4-34-57

30. Амосов А.П., Титова Ю.В., Уварова И.А., Белова Г.С. Азидный самораспространяющийся высокотемпературный синтез высокодисперсной порошковой композиции AlN–SiC с применением политетрафторэтилена. *Известия вузов. Порошковая металлургия и функциональные покрытия*. 2024;18(6):28–43. https://doi.org/10.17073/1997-308X-2024-6-28-43

Amosov A.P., Titova Yu.V., Uvarova I.A., Belova G.S. Azide self-propagating high-temperature synthesis of a highly dispersed AlN–SiC powder composition using polytetrafluoroethylene. *Powder Metallurgy and Functional Coatings*. 2024; 18(6):28–43. https://doi.org/10.17073/1997-308X-2024-6-28-43

31. Uvarova I.A., Amosov A.P., Titova Yu.V., Novikov V.A. Self-propagating high-temperature synthesis of a highly dispersed Si_3N_4–SiC ceramic powders composition using sodium azide and polytetrafluoroethylene. *Powder Metallurgy and Functional Coatings*. 2025;19(3):25–38. https://doi.org/10.17073/1997-308X-2025-3-25-38

Уварова И.А., Амосов А.П., Титова Ю.В., Новиков В.А. Самораспространяющийся высокотемпературный синтез высокодисперсной композиции керамических порошков Si_3N_4–SiC с применением азида натрия и политетрафторэтилена. *Известия вузов. Порошковая металлургия и функциональные покрытия*. 2025;19(3):25–38. https://doi.org/10.17073/1997-308X-2025-3-25-38

32. Khachatryan G.L., Arutyunyan A.B., Kharatyan S.L. Activated combustion of a silicon–carbon mixture in nitrogen and SHS of Si_3N_4–SiC composite ceramic powders and silicon carbide. *Combustion, Explosion, and Shock Waves*. 2006;42(5):543–548. https://doi.org/10.1007/S10573-006-0086-7

Хачатрян Г.Л., Арутюнян А.Б., Харатян С.Л. Активированное горение смеси кремний–углерод в азоте и СВС композиционных керамических порошков Si_3N_4/SiC и карбида кремния. *Физика горения и взрыва*. 2006;42(5):56–62.

33. Amirkhanyan N., Kirakosyan H., Zakaryan M., Zurnachyan A., Rodriguez M.A., Abovyan L., Aydinyan S. Sintering of silicon carbide obtained by combustion synthesis. *Ceramics International*. 2023;49(15):26129–26134. https://doi.org/10.1016/j.ceramint.2023.04.233

34. Amosov A.P., Belova G.S., Titova Yu.V., Maidan D.A. Synthesis of highly dispersed powder ceramic composition Si_3N_4–SiC by combustion of components in the Si–C–NaN_3–NH_4F system. *Russian Journal of Inorganic Chemistry*. 2022;67(2):123–130. https://doi.org/10.1134/S0036023622020024

Амосов А.П., Белова Г.С., Титова Ю.В., Майдан Д.А. Синтез высокодисперсной порошковой керамической композиции Si_3N_4–SiC при горении компонентов в системе Si–C–NaN_3–NH_4F. *Журнал неорганической химии*. 2022;67(2):139–147. https://doi.org/10.31857/S0044457X22020027

35. Amosov A.P., Bichurov G.V. Azide technology of self-propagating high-temperature synthesis of micro- and nanopowders of nitrides. Moscow: Mashinostroenie-1, 2007. 526 p. (In Russ.).

Амосов А.П., Бичуров Г.В. Азидная технология самораспространяющегося высокотемпературного синтеза микро- и нанопорошков нитридов. М.: Машиностроение-1, 2007. 526 с.

Information about the Authors

Irina A. Uvarova – Engineer of the Department of Metallurgy, Powder Metallurgy, Nanomaterials (MPMN), Samara State Technical University (SamSTU)
ORCID: 0000-0003-3023-3289
E-mail: mr.simple2@mail.ru

Aleksandr P. Amosov – Dr. Sci. (Phys.-Math.), Professor, Head of the Department of MPMN, SamSTU
ORCID: 0000-0003-1994-5672
E-mail: egundor@yandex.ru

Yuliya V. Titova – Cand. Sci. (Eng.), Associate Professor of the Department of MPMN, SamSTU
ORCID: 0000-0001-6292-280X
E-mail: titova600@mail.ru

Сведения об авторах

Ирина Александровна Уварова – инженер кафедры «Металловедение, порошковая металлургия, наноматериалы» (МПМН), Самарский государственный технический университет (СамГТУ)
ORCID: 0000-0003-3023-3289
E-mail: mr.simple2@mail.ru

Александр Петрович Амосов – д.ф.-м.н., профессор, заведующий кафедрой МПМН, СамГТУ
ORCID: 0000-0003-1994-5672
E-mail: egundor@yandex.ru

Юлия Владимировна Титова – к.т.н., доцент кафедры МПМН, СамГТУ
ORCID: 0000-0001-6292-280X
E-mail: titova600@mail.ru

Anton A. Ermoshkin – Cand. Sci. (Eng.), Head of the Testing Center of IT-Service LLC
ORCID: 0009-0005-6679-7133
E-mail: nerev89@yandex.ru

Антон Александрович Ермошкин – к.т.н., начальник Испытательного центра ООО «ИТ-Сервис»
ORCID: 0009-0005-6679-7133
E-mail: nerev89@yandex.ru

Contribution of the Authors

I. A. Uvarova – conducted combustion-mode synthesis experiments on powder compositions; prepared and formatted experimental results; participated in the analysis and discussion of the findings; contributed to writing the manuscript.
A. P. Amosov – defined the research objective; summarized the obtained results; wrote and edited the manuscript.
Yu. V. Titova – formulated the research tasks; planned the experiments; analyzed and discussed the results; contributed to writing the manuscript.
A. A. Ermoshkin – performed XRD analyses of synthesized powder compositions, participating in the analysis and discussion of the results.

Вклад авторов

И. А. Уварова – проведение экспериментов по синтезу порошковых композиций в режиме горения, подготовка и оформление результатов экспериментов, участие в анализе и обсуждении результатов, участие в написании статьи.
А. П. Амосов – определение цели работы, обобщение полученных результатов, написание и редактирование текста статьи.
Ю. В. Титова – постановка задач исследований, планирование экспериментов, анализ и обсуждение результатов, участие в написании статьи.
А. А. Ермошкин – проведение РФА-исследований синтезированных порошковых композиций, участие в анализе и обсуждении результатов.

Received 20.06.2025
Revised 11.08.2025
Accepted 18.08.2025

Статья поступила 20.06.2025 г.
Доработана 11.08.2025 г.
Принята к публикации 18.08.2025 г.